

Understanding the significance of sample preparation in studies of the nanoparticle metabolite corona

Zhang, Wei; Chetwynd, Andrew J.; Thorn, James A.; Lynch, Iseult; Ramautar, Rawi

DOI:

[10.1021/acsmeasuresciau.2c00003](https://doi.org/10.1021/acsmeasuresciau.2c00003)

License:

Creative Commons: Attribution-NonCommercial-NoDerivs (CC BY-NC-ND)

Document Version

Publisher's PDF, also known as Version of record

Citation for published version (Harvard):

Zhang, W, Chetwynd, AJ, Thorn, JA, Lynch, I & Ramautar, R 2022, 'Understanding the significance of sample preparation in studies of the nanoparticle metabolite corona', *ACS Measurement Science Au*.
<https://doi.org/10.1021/acsmeasuresciau.2c00003>

[Link to publication on Research at Birmingham portal](#)

General rights

Unless a licence is specified above, all rights (including copyright and moral rights) in this document are retained by the authors and/or the copyright holders. The express permission of the copyright holder must be obtained for any use of this material other than for purposes permitted by law.

- Users may freely distribute the URL that is used to identify this publication.
- Users may download and/or print one copy of the publication from the University of Birmingham research portal for the purpose of private study or non-commercial research.
- User may use extracts from the document in line with the concept of 'fair dealing' under the Copyright, Designs and Patents Act 1988 (?)
- Users may not further distribute the material nor use it for the purposes of commercial gain.

Where a licence is displayed above, please note the terms and conditions of the licence govern your use of this document.

When citing, please reference the published version.

Take down policy

While the University of Birmingham exercises care and attention in making items available there are rare occasions when an item has been uploaded in error or has been deemed to be commercially or otherwise sensitive.

If you believe that this is the case for this document, please contact UBIRA@lists.bham.ac.uk providing details and we will remove access to the work immediately and investigate.

Understanding the Significance of Sample Preparation in Studies of the Nanoparticle Metabolite Corona

Wei Zhang,* Andrew J. Chetwynd,* James A. Thorn, Iseult Lynch, and Rawi Ramautar

Cite This: <https://doi.org/10.1021/acsmeasuresciau.2c00003>

Read Online

ACCESS |



Metrics & More



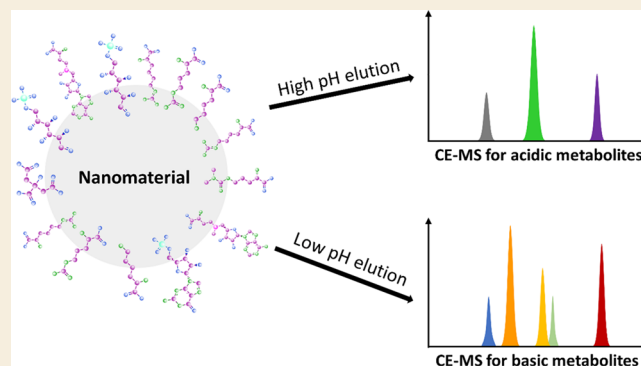
Article Recommendations



Supporting Information

ABSTRACT: The adsorption of metabolites to the surface of nanomaterials is a growing area of interest in the field of bionanointeractions. Like its more-established protein counterpart, it is thought that the metabolite corona has a key role in the uptake, distribution, and toxicity of nanomaterials in organisms. Previous research has demonstrated that nanomaterials obtain a unique metabolite fingerprint when exposed to biological matrices; however, there have been some concerns raised over the reproducibility of bionanointeraction research due to challenges in dispersion of nanomaterials and their stability. As such, this work investigates a much-overlooked aspect of this field, i.e., sample preparation, which is vital to the accurate, reproducible, and informative analysis of the metabolite corona. The impact of elution buffer pH, volume, and ionic strength on the metabolite corona composition acquired by uncapped and polyvinylpyrrolidone (PVP)-capped TiO₂ from mixtures of cationic and anionic metabolites was studied. We demonstrate the temporal evolution of the TiO₂ metabolite corona and the recovery of the metabolite corona, which resulted from a complex biological matrix, in this case human plasma. This work also demonstrates that it is vital to optimize sample preparation for each nanomaterial being investigated, as the metabolite recovery from Fe₃O₄ and Displex-capped TiO₂ nanomaterials is significantly reduced compared to the aforementioned uncapped and PVP-capped TiO₂ nanomaterials. These are important findings for future bionanointeraction studies, which is a rapidly emerging area of research in nanoscience.

KEYWORDS: capillary electrophoresis, mass spectrometry, nanoparticles, nanomaterials, sample preparation, metabolite corona



1. INTRODUCTION

The field of bionanointeractions explores how biological molecules in the environment interact with nanomaterials (NMs) and has been an intense area of research for more than a decade.^{1,2} This field has been dominated by investigation of the protein corona, the name given to the layer of proteins that adsorb to the surface of NMs. It has been demonstrated that these proteins have a profound effect upon the uptake, distribution, and biological pathways activated in response to NM exposures to humans, other animals, and plants.^{1,3,4} However, the diversity of other molecules found in biological matrices has for the most part been overlooked, although there is growing evidence that other biomolecules such as nucleic acids,^{5,6} lipids,^{7,8} and metabolites^{9–12} are also recruited into the corona, making the term biomolecular corona a more representative name for the complexity of the biomolecules interacting with NMs. This biomolecular corona has been demonstrated to influence the stability, biodistribution, and toxicity of NMs in human/environmental health and disease.^{1,3} Thus, it has become an important field of research to help understand how NMs impact the health and wellbeing of

humans and the environment into which NMs are released either intentionally or through waste mismanagement.

In recent years, there has been increasing interest in the role of metabolites in the biomolecular corona.^{9–13} These metabolites are orders of magnitude smaller than proteins, being typically less than 1000 Da; however, as with proteins, they can interact with intercellular and intracellular receptors and thus have the potential to impact the distribution and toxicity of NMs.^{12,13} Early studies investigating lipids, a subset of the metabolome, have shown that they influence the biological response to NMs.¹⁴ As with the protein corona, it has also been shown that NMs adsorb a unique metabolite fingerprint^{9–12} that is matrix specific^{7,9,12} and that NM surface chemistry provides specificity to the composition of metabolite coronas.¹⁵ It has also been demonstrated that proteins in the

Received: January 17, 2022

Revised: February 4, 2022

Accepted: February 7, 2022

corona impact the adsorption of metabolites.¹⁰ As such there is a significant need for further research to understand the mechanisms of metabolite binding to NMs and their impact on the stability, dissolution, and biological interactions of the metabolite corona.

In recent years, there have been concerns over the reproducibility and reporting of NM-based research^{16,17} with specific concerns being raised over the reproducibility of protein corona studies due to incomplete reporting of the sample preparation, extraction, and analysis steps.¹⁸ It is also recognized that sample preparation is frequently overlooked in the broader field of metabolomics despite it being a crucial aspect for reproducibility and sensitivity.¹⁹ As a result, sample preparation is key to understanding the hurdles posed to the isolation and analysis of the metabolites from the NM corona in these early stages of development and optimization of the methodologies and workflow for investigation of this aspect of bioanointeractions. In the case of the protein corona, relatively few studies have systematically investigated the impact of sample preparation and approaches used for recovery of proteins from the protein corona on the identified corona composition,^{20–23} despite a number of approaches being used such as on-particle,^{20,21} in-solution,^{20,21} in-gel²¹ digests or sucrose cushion²² to strip the corona from the NMs for proteomics analysis. As a result, no single method dominates the protein corona field and the vast majority of studies did not consider validation of the methods used to ensure maximum recovery and reproducibility of protein corona characterization. This may have resulted in bias being introduced into studies where some proteins were preferentially isolated and analyzed, leading to an inaccurate representation of the content of the protein corona and the correlations between NM properties and acquired corona compositions.³

In the case of the metabolite corona, there is a higher proportion of studies investigating the impact of test conditions due to the smaller body of research to date. Grntzalis et al. investigated amino-capped polystyrene particles and evaluated the recovery of metabolites using a single molecule, SDS. In this work, fine tuning of the extraction method was required to minimize experimental variance; however, this was limited to a single NM and single metabolite molecule and thus may not scale up to general applicability.¹¹ Pink et al. dissolved the particles to recover everything bound to the NMs (copper oxide, titanium dioxide, zinc oxide, zirconium dioxide, and carbon black) though no recovery study was reported.⁹ Lee et al. carried out an extensive program to determine the recovery of lipids from three different NMs and demonstrated a recovery greater than 80% for their optimized method for TiO₂ NMs and cellulose nanofibril particles but only 50% for polystyrene, with lipid-dependent recovery observed.⁷ This offers two key insights: a singular extraction method may not apply across all NMs, and it will also be essential to screen for more than one metabolite species in a recovery study to ensure a broad applicability.

In the current work, a solvent-based elution protocol was initially developed using two TiO₂ NMs, namely, uncapped and polyvinylpyrrolidone (PVP)-capped TiO₂, which were shown in previous work¹⁰ to adsorb the most cationic and anionic metabolites from standard mixtures. Different solvents, pH, and elution periods were assessed using the uncapped (cations) and PVP-capped (anions) TiO₂ NMs in order to assess the impact of these parameters on recovery, and then, an optimized protocol was applied to two other NMs (Dispex-

capped TiO₂ NMs and uncapped Fe₃O₄ NMs) to assess its general applicability. The metabolites selected for this work are all highly charged and polar metabolites covering amino acids, amines, sugar phosphates, organic acids, and nucleotides. These encompass monomers of proteins and nucleic acids, which are known to adsorb to NMs^{9–11} in addition to other metabolites encompassing a wide chemical space, which have either previously been seen to adsorb to NMs or cover key metabolite classes. Due to the highly charged and polar nature of the metabolites, they were analyzed using sheathless capillary zone electrophoresis mass spectrometry (CE-MS).^{24,25} This approach is well-suited for the selective and sensitive profiling of polar ionogenic compounds in a wide range of matrices^{26,27} and has been successfully applied to NM research²⁸ and protein^{21,29} and metabolite corona^{10,29} analysis, with recent work showing excellent reproducibility for metabolomics.³⁰ This work offers a basis for future studies investigating the polar metabolites present in the biomolecular corona acquired by NMs in complex biofluids, enabling high reproducibility and high recoveries, to ensure that accurate and reliable metabolite corona analysis can be performed.

2. MATERIALS AND METHODS

Metabolite standards were supplied by Sigma-Aldrich (St Louis, MO, USA), Fluka (Steinheim, Germany), Cortecnet (Voisins Le Bretonneux, France), Cambridge Isotope Laboratories (Andover, MA, USA), Calbiochem (Nottingham, UK), Alfa Aesar (Ward Hill, MA, USA), and Roth (Karlsruhe, Germany). Centrifugal ultrafilters (3 kDa cutoff membrane) were purchased from Merck. Acetic acid (99–100%) was purchased from VWR (Amsterdam, The Netherlands). Water used in this work was acquired from a Milli-Q Advantage A10 water purification system (Millipore, Amsterdam-Zuidoost, The Netherlands). For quantification, three internal standards (ISTDs) were used for cationic analysis, including DL-methionine sulfone, N-methyl-d3-L-histidine, and L-d4-lysine (2–4 μM final concentration), and two ISTDs were used for anionic profiling, including D-13C6-glucose-6-phosphate and 2,2,4,4-d4-citric acid (40 μM final concentration). Pooled human plasma, anticoagulated with EDTA, was obtained from Sanquin Blood Bank (Leiden, The Netherlands).

Three anatase titanium dioxide (TiO₂) NMs with the same primary particle size (13 nm) but different capping states (uncapped, denoted as TiO₂-un), PVP-capped (denoted as TiO₂-PVP), and Dispex AA4040 capped (denoted as TiO₂-DISPEX) were sourced from Promethean Particles Ltd. (Nottingham, UK). Uncapped Fe₃O₄ NMs with a primary particle size of 100 nm were also purchased from Promethean Particles Ltd.

2.1. NM Characterization

This study builds upon our previous investigation of the interaction characteristics between polar metabolites and NMs. The emphasis of the current work is the evaluation of elution procedures for better recovery of compounds bound to NMs. The three anatase titanium dioxide NMs were used in our previous studies and have been characterized in terms of their core size by hydrodynamic size and zeta potential by dynamic light scattering (DLS).^{10,21,31} DLS characterization of the uncapped Fe₃O₄ NMs was performed in MilliQ water.

2.2. Incubation of NMs with Metabolite Standards in Water

Two standard mixes of metabolites (45 cations and 7 anions) were selected and prepared for incubation experiments. Incubation experiments were conducted in water using a fixed NM concentration (1 mg/mL). All metabolites in the two mixes are detailed in Tables S1 and S2, and physical and chemical properties are obtained from the human metabolome database.³² The preparation of some of the standard solutions involved the addition of formic acid, ammonia,

and/or methanol. Hence, to eliminate any potential interferences caused by undesired chemical components, the standard solutions were first added to clean Eppendorf tubes intended for incubation, and the solvents evaporated in a SpeedVac concentrator (Labconco, Kansas, MO, USA) before the experiments. The stocks of NMs were subjected to sonication in a water bath (Branson 5510) for 2 min prior to addition into the incubation mixes. In parallel to incubation with the presence of NMs, control samples were prepared to evaluate the stability of the standards under the same incubation conditions. Incubation was conducted with an incubating microplate shaker (VWR, The Netherlands) at 37 °C with mixing at 800 RPM. Calibration curves for compounds were constructed for quantitative studies over the range of 0.25–3.125 μM for cations and 1–12.5 μM for anions in water unless otherwise noted.

Into the Eppendorf tubes pre-coated with standards, corresponding amounts of NM solutions and water were added and the vials were vortexed for 2 min in a VX-2500 Multi-Tube Vortexer (VWR, The Netherlands) before the samples were placed into the incubating microplate shaker. The final incubation mix contained a fixed concentration of NM at 1 mg/mL. Two different TiO_2 NMs, based on their adsorption capability for cationic and anionic compounds separately as determined in our previous studies,¹⁰ were selected for screening of the optimal wash procedures. For incubation experiments with cations, TiO_2 -un was used as a model NM with the final concentration of cationic compounds being 2.5 μM . To demonstrate the time-dependent interaction characteristics between NMs and metabolites, the cationic incubation experiments were investigated closely over different incubation durations, namely 0, 30, 60, and 90 min. For incubation studies with anions, TiO_2 -PVP was chosen as a representative NM with anionic compounds present in the mix at 10 μM . The final volume for incubation experiments was 300 μL . After incubation, the samples were immediately centrifuged at 21,000 g at 4 °C for 10 min. The supernatant was transferred and filtered through centrifugal filters with a 3 kDa cutoff membrane (Merck Millipore, Billerica, MA, USA), after which 75 μL of the filtrate was taken and the solvent evaporated to dryness. The dried samples were stored at –20 °C prior to analysis. All samples were prepared in triplicate.

2.3. Influence of pH of Elution Buffers on Metabolite Recovery

After transferring the supernatant out of the incubation mix, the residual liquid was removed from the NM pellets. The optimization of elution procedures was conducted separately for cations and anions. The elution of cationic metabolites made use of a 10 mM ammonium formate solution, with its pH value adjusted to 3, 4, 9, and 10 with either formic acid or ammonia. For the elution optimization of anionic metabolites, two different solutions were used, namely, 10 mM ammonium formate (pH 4, 9, and 10) and 10 mM ammonium bicarbonate (pH 10.9) on the basis of the useful ranges of different buffers. The elution was realized by adding 300 μL of the aforementioned solutions followed by rigorous pellet dispersion with a bullet blender (Next Advance, Inc. Troy, NY) for 2 min and sonication in a water bath at room temperature for 4 min. Afterwards, the samples were subjected to a 15 s vortex before they were centrifuged at 21,000 g at 4 °C for 10 min. The following steps were the same as described in the previous section (Section 2.2), including supernatant transfer, centrifugal ultrafiltration, and solvent evaporation.

Once the optimized conditions were determined, their effects were further tested with the other two NMs, namely, TiO_2 -DISPEX and uncapped Fe_3O_4 . The incubation experiments in the step utilized both cations and anions in the same incubation mix, with their concentrations being 2.5 and 5 μM , respectively, while the final concentration of NMs remained unchanged. After the supernatant was transferred for further processing and residual liquid was removed from the pellets, the elution was achieved with the addition of both elution solutions in a two-step elution process, where the optimized cation elution was performed first followed by the optimized anion elution in sequence. After both elute fractions were ultrafiltered, equal volumes (the same as the incubation supernatant) from each filtrate

were collected and combined followed by solvent evaporation and storage at –20 °C before analysis. For the analysis of samples acquired from various NMs, a pooled QC sample was generated by combining 5 μL of every reconstituted sample and analyzed repeatedly across the CE-MS sequence.

2.4. Influence of the Volume and Ionic Strength of Elution Solutions on Anion Recovery

To investigate whether a larger volume of elution solution could affect the recovery of anions, 300 and 600 μL of 10 mM ammonium formate solutions (pH 10.0) were chosen for comparison for their elution effects of anions from TiO_2 -PVP pellets after incubating with a 10 μM concentration of the anion standards. The difference in the elution volumes was compensated for by collecting twice the volume of elution fraction filtrate after ultrafiltration when eluting with 600 μL compared to that obtained from elution with 300 μL . The solvents were then evaporated to dryness and stored at –20 °C.

In order to examine the effect of the ionic strength of elution solutions on the recovery of anionic compounds, the NM pellets after incubation were subjected to elution with either a 10 mM ammonium formate or a 50 mM ammonium formate solution of the same pH (10.0). To induce more adsorption of anions to NMs, a lower final concentration of anions (5 μM) was used for this evaluation. The handling of the incubation supernatant and elution fractions was as described above.

2.5. Incubation of NMs and Cationic Metabolites with Intact Human Plasma

To investigate whether the proposed elution procedure is applicable for NMs incubated with the presence of more complex biological matrices, incubation experiments were conducted with three different NMs, namely, uncapped TiO_2 , TiO_2 -DISPEX, and Fe_3O_4 NMs, using intact human plasma as a model matrix (Table S3). All the tubes used for incubation study were first spiked with cationic standards as described in Section 2.2, and the solvent was evaporated to dryness. The subsequent incubation mix consisted of 5 μL of human plasma, water, and different types of NMs (1 mg/mL)/no NM (control group) with a final volume of 300 μL . To enable more accurate pipetting of human plasma, the pooled plasma was initially diluted 10 times with water. The subsequent procedures including vortex, incubation, and centrifugation were performed as previously described (Section 2.2). After centrifugation, 250 μL of the supernatant was transferred to clean Eppendorf tubes where 200 μL of methanol, 50 μL of ISTD solutions (containing 6 μM DL-methionine sulfone, N-methyl-d3-L-histidine, and L-d4-lysine in methanol), and 250 μL of CHCl_3 were later added. The samples were subjected to vortex for 2 min followed by centrifugation at 21,000 g at 4 °C for 10 min. Then, 450 μL of the supernatant after centrifugation was then transferred to centrifugal filters with a 3 kDa cutoff membrane. Following this, 330 μL of filtrate was obtained and placed in clean vials for solvent evaporation.

For metabolite elution, the process was similar to that described for incubation experiments without biological matrices, featuring the addition of elution solution, pellet dispersion, sonication, and centrifugation. However, the acquired supernatant was subjected to the same liquid–liquid extraction as its incubation supernatant. For the analysis of the samples, 35 μL of water was added to each dried sample and thoroughly vortexed before 5 μL was taken from each sample (except for calibration curve samples) and combined as the QC sample, which was analyzed for every six samples in the CE-MS sequence.

2.6. Analysis of Metabolites by Sheathless CE-MS

The separation of the prepared samples was conducted with a CESI 8000 Plus instrument from SCIEX (Brea, CA, USA) with an OptiMS CESI cartridge (30 μm ID \times 91 cm bare fused silica capillary) thermostatted at 25 °C. The coupling of the CE instrument to an SCIEX TripleTOF 6600 MS system was achieved with a NANOSpray III source. Electrospray ionization (ESI) was performed in positive ion mode for cations and negative ion mode for anions, with the porous tip of the capillary positioned 3–4 mm from the entrance of

Table 1. Physical Characteristics of Study Nanomaterial Dispersions at 5 mg/mL in MilliQ Water

| nanomaterial | hydrodynamic diameter (nm) | polydispersity index | zeta potential (mV) | electrophoretic mobility ($\mu\text{m cm Vs}$) |
|--------------------------------|----------------------------|----------------------|---------------------|--------------------------------------------------|
| TiO ₂ -un | 922.3 \pm 81.3 | 0.07 \pm 0.05 | 24.2 \pm 1.3 | 1.9 \pm 0.1 |
| TiO ₂ -DISPEX | 17,578.7 \pm 793.4 | 0.27 \pm 0.16 | 24.85 \pm 1.5 | 2.0 \pm 0.1 |
| TiO ₂ -PVP | 2076.2 \pm 666.7 | 0.58 \pm 0.32 | 84 \pm 1.1 | 0.65 \pm 0.1 |
| Fe ₃ O ₄ | 136.8 \pm 2.1 | 0.24 \pm 0.01 | -46.7 \pm 1.7 | -3.7 \pm 0.1 |

the MS inlet. Detailed descriptions of the analytical methods employed were provided in previous studies.^{10,29,33} Optimal IonSpray Voltage Floating values were determined with manual tuning to be in the range of 1350–1550 V for ESI-MS positive ion mode and 1400–1600 V for negative ion mode. The conditioning of new capillaries and rinsing between runs were performed as previously described.^{10,29} The dried samples (except for samples prepared with plasma) were reconstituted in 35 μL of ISTD solutions, and 20 μL of supernatants after centrifugation at 21,000 g at 4 °C for 10 min were placed into nanoVials (SCIEX). The sample tray was thermostatted at 10 °C. All samples were injected hydrodynamically (at 2 psi for 20 s for cations and 15 s for anions, corresponding to 0.7% of the capillary volume or about 4.6 nL and 0.5% and 3.5 nL, respectively) and separated with 10% acetic acid (pH 2.2) as the background electrolyte. A voltage of 30 kV was used for electrophoretic separation, and an inner pressure of 1 psi was applied during the separation of anions. Full scan MS data acquisition covered the mass range from 65 to 1000 m/z .

2.7. Data Analysis

The peak integration and concentration quantification was conducted within MultiQuant 3.0.3 (SCIEX, Brea, CA, USA). Paired t-test and ANOVA analyses were conducted in GraphPad Prism version 8.1.1 for comparing metabolite adsorption and elution fraction development. For samples prepared with human plasma, the peak areas were first integrated in MultiQuant and QC samples were checked for their relative standard deviation (RSD) values. Only compounds with RSD values below 30% were subjected to multivariate analyses in SIMCA (Simca 17, Umetrics, Umeå, Sweden). The cases were missing, values were seen within replicates, the mean was used as a replacement, and this only occurred twice during this work where the detected concentration was very low.

3. RESULTS AND DISCUSSION

3.1. Nanoparticle Characterization

The TiO₂ NMs have been characterized in our previous work on both the protein and metabolite corona,^{10,21,31} and their properties are detailed in Table 1 alongside the particle that is new to this work, Fe₃O₄, which was characterized at 4 mg/mL in deionized MilliQ water. The Fe₃O₄ retains a size similar to the primary manufactured size of the particles though with a relatively large degree of polydispersity. The TiO₂ NMs however show significant aggregation and agglomeration, though this also may reflect the nonspheroid shape of the particles, which is a limiting factor of DLS.

3.2. Metabolite Stability

A key aspect to corona studies is the incubation of NMs in a biological matrix typically at human body temperature for an extended period of time. A potential risk associated with this is that the metabolites may undergo thermal or photo degradation and thus skew the resulting metabolite corona interpretation. In this work, for the cations, all 45 were incubated at 2.5 μM for 90 min at 37 °C, and then, concentrations were quantified using CE-MS. Across all cations, the average percentage of total remaining after 90 min was 100.09 \pm 2.81%, demonstrating excellent stability across the range of metabolites (data not shown). The seven anions were incubated at 10 μM for 60 min at 37 °C; shorter

time periods were used, as their stability is a known issue, and a higher concentration is used due to the difficulty in ionizing these metabolites. After the incubation, on average 100.98 \pm 1.64% of the anions remained present, again demonstrating excellent stability over the time course of a typical incubation. Both sets of metabolites showed only variation that would be accepted as analytical variation in the measurements, with an average RSD for all cation triplicates of 2.03% and anions of 2.8%. These findings suggest that the metabolites do not degrade during a typical incubation experiment, meaning that future studies on the metabolite corona can mirror the incubation settings of a typical protein corona analysis with confidence or even perform protein and metabolite analysis together to quantify both the protein and metabolite corona of the same sample.

3.3. Influence of pH of Elution Solutions on Metabolite Recovery

The pH of wash/elution solutions is a well-known property impacting the recovery of metabolites from particles in particular during solid-phase extraction^{34,35} and affects column chemistries in liquid chromatography.³⁶ Given that both these technologies are based upon particle chemistries in much the same way as the corona is formed around NMs, investigating similar methods for metabolite recovery is vital. In this study, a CE-MS compatible solvent, 10 mM ammonium formate, was tested at four pH levels for cations (i.e., pH 3, 4, 9, and 10) and for anions (pH 4, 9, 10, and 10.9). Initially, the methods were tested using the uncapped TiO₂ and PVP-capped TiO₂ NMs separately, to allow a greater range of method variables to be tested. It is therefore imperative to use NMs that adsorb many metabolites for this screening process in order to better illustrate the ability of the elution solutions to remove a wide range of metabolites from the NMs.

3.3.1. Cation Recovery. It is evident that the pH of the elution solution plays a clear role in the recovery of metabolites recruited to the metabolite corona (Figure 1). The two basic pHs studied, pH 9 and 10, performed the worst with on average 45.4 and 48.1% recovery, respectively, of the 23 metabolites evaluated. Specifically, only six cations had no significant differences between pH values evaluated ($p > 0.05$). The two acidic pHs (pH 3 and 4) returned significantly higher recoveries ($p < 0.05$ to $p < 0.0001$) than either of the basic pHs for 15 cations. This is likely due to the high pH levels leading to a higher proportion of charged metabolites; thus, they remain adsorbed to the surface of the NMs. The acidic pHs are more likely to produce neutral forms of the analytes, thus disrupting the chemical bonding between the metabolite and NM surface, therefore enhancing their desorption from the NMs.^{34,35} The performance of the two acidic solvents was very similar to the average recovery being 70.7 and 68.4 for pH 3 and 4, respectively. The solvent buffered to pH 3 performed up to 2 times better for some of the lowest recovery metabolites, SAM and SAH, and over all metabolites allowed for a more reproducible analysis with the average RSD at pH 3 being 4.6% vs 6.3% for the pH 4 solution. Due to the high rates of recovery

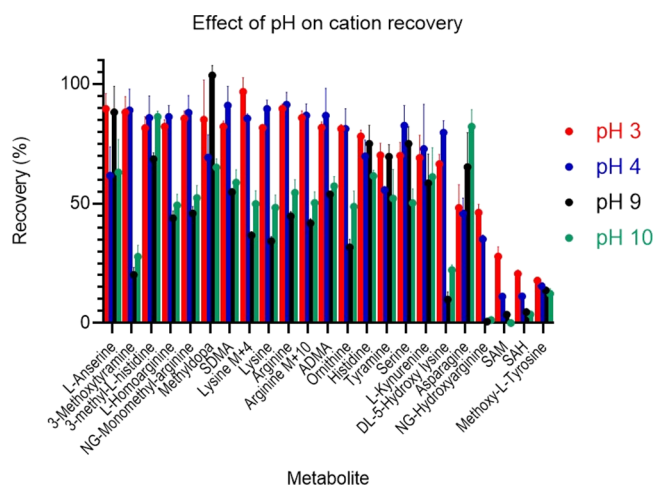


Figure 1. Effect of elution buffer pH on recovery of cations from corona acquired by uncapped TiO_2 NMs.

and reproducibility for the cations using pH 3, no further optimization was performed for the recovery of cationic metabolites.

3.3.2. Anion Recovery. As with the cations, the recovery of anions is equally dependent upon the pH of the elution solution (Figure 2). Due to the pK_a of the anions, it is expected

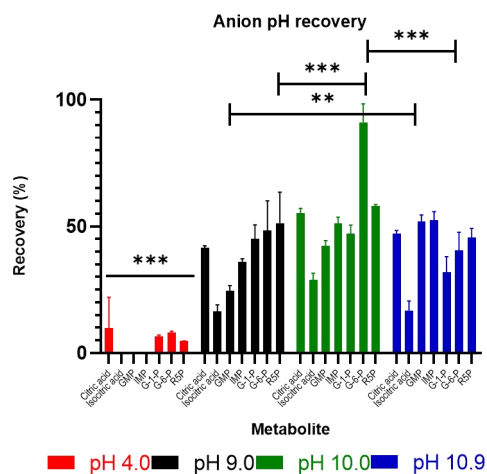


Figure 2. Effect of elution buffer pH on recovery of anions from PVP-capped TiO_2 NMs. ** = $p < 0.01$; *** = $p < 0.001$.

that a higher pH wash will return higher recovery rates for these metabolites. This is reflected in the data generated from this experiment, whereby only the acidic pH, pH 4.0, demonstrated very poor recoveries of the anions with isocitric acid, GMP, and IMP not being recovered at all and no anion having an average recovery $>10\%$. Every metabolite had a significantly lower ($p < 0.0001$) recovery at pH 4.0 than under the other three conditions tested. As a result, the other three pHs evaluated were basic at pH 9.0, 10.0, and 10.9 to alleviate the issues of low recovery at acidic pH. The basic conditions performed similarly across the seven anions with glucose-6-phosphate having a significantly greater ($p < 0.001$) recovery at pH 10.0 compared to 9.0 and 10.9 and pH 10.9 showing a significantly greater ($p < 0.01$) recovery for guanosine monophosphate (GMP) than pH 9.0. There is also a general trend, as seen in Figure 2, that pH 10.0 performs slightly better

across the range of metabolites, and as such, this was chosen for the subsequent anion experimentation.

There also arise interesting comparisons between the isomers present in the anion mixture; looking solely at the pH 10.0 data, there are significant differences between citric and isocitric acid ($p < 0.01$) with a 1.9 fold difference in recovery and G-1-P and G-6-P ($p < 0.05$) also have a 1.9 fold difference in recovery. These reflect the differences seen in the adsorption of these metabolites to the metabolite corona as was shown in previous work.¹⁰ This suggests that the mechanism behind the adsorption of these isomers differs and warrants further work to understand the mechanism of their adsorption and how this may impact the uptake, distribution, and toxicity of NMs.¹⁰

3.4. Influence of the Volume and Ionic Strength of Elution Solutions on Anion Recovery

Due to the relatively low anion recoveries observed at the optimal solvent pH 10.0, further properties of the elution solvent were optimized. Initially, the volume was investigated to ensure that an adequate volume was present to fully resolubilize the anionic metabolites; however, using a 600 μL volume did not reliably increase recoveries of the anions compared to the initial 300 μL used previously (Table S4). The only noticeable differences to be observed were for glucose-1-phosphate and glucose-6-phosphate where the amount of metabolite recovered improved by up to 20%. However, this came at the expense of recovery reproducibility where the RSD increased to $>20\%$, making the method too unreliable to carry forward. Thus, 300 μL of solvent was used for subsequent analysis.

The last property of the elution buffer to be evaluated was the ionic strength, which, alongside pH, affects the charge state of the metabolite (Figure 3). Here, 10 mM ammonium

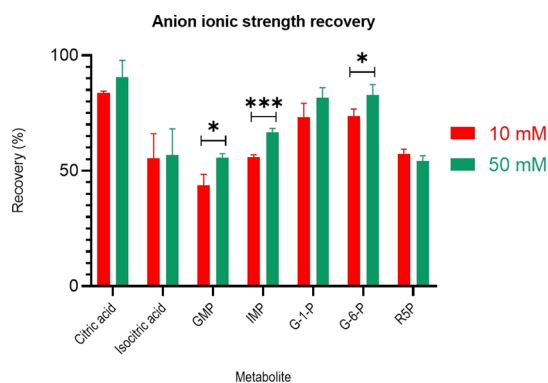


Figure 3. Recovery of anions from PVP-capped TiO_2 with different ionic strength elution buffers. * = $p < 0.05$; *** = $p < 0.001$.

formate was compared to 50 mM ammonium formate for the seven anions. As can be seen in Figure 3, the higher ionic strength significantly increased ($p < 0.05$) the recovery of GMP, IMP, and glucose-6-phosphate. The overall average recovery increased from 63.3 to 69.8% with the higher ionic strength elution solution. However, the increased ionic strength of the buffer could potentially lead to very unstable currents, which can impact migration time stability, spray stability, and subsequently peak area reproducibility, while also potentially reducing the longevity of the capillary. As such, the remaining anionic work presenting in this study continues to use a 10 mM solution. However, for a non-CE-based analysis

such as liquid chromatography or gas chromatography, this higher ionic strength buffer may be a more optimal approach, as those methods do not rely upon electrical conductivity.

3.5. Temporal Evolution of the Metabolite Corona

It is well established that over time the protein corona composition undergoes dynamic changes whereby high abundance, low affinity proteins are exchanged for high affinity, low abundance proteins.^{37–39} In the current work, the newly developed metabolite corona isolation method is applied to determine if and how the metabolite corona undergoes dynamic changes over a time course experiment. Here, cations were incubated for 0, 30, 60, and 90 min with uncapped TiO₂ NMs and the metabolite corona composition was quantified (Table 2). Due to the small number of anions

Table 2. Significant Percentage Change in Metabolite Corona of Uncapped TiO₂ NMs, Determined from the Total Quantification at Each Time Point, Evaluated over 90 min^a

| metabolite | time period (min) | | | | | |
|---------------------|-------------------|------|------|-------|-------|-------|
| | 0–30 | 0–60 | 0–90 | 30–60 | 30–90 | 60–90 |
| 3-methoxytyramine | 5% | ns | 74% | 72% | ns | ns |
| DL-5-hydroxy lysine | Ns | 61% | ns | 53% | ns | ns |
| L-anserine | Ns | ns | ns | 13% | 9% | ns |
| methoxy-L-tyrosine | Ns | ns | 11% | 4% | ns | ns |
| O-acetyl-L-serine | 52% | 74% | 85% | 45% | ns | ns |
| ornithine | Ns | 33% | ns | 27% | ns | ns |
| serotonin | 81% | ns | 91% | 76% | 88% | 49% |
| tyramine | Ns | 17% | 15% | 15% | ns | ns |
| arginine | Ns | 26% | ns | 19% | ns | ns |

^aPercentages represent significant changes ($p < 0.05$) in metabolite concentration in the corona, positive numbers represent an increase in concentration, a negative value demonstrates a drop in concentration, and ns denotes that any changes observed were not significant.

evaluated in this work, their temporal evolution was not evaluated. Of the 45 cations investigated, 9 showed significant variation over the length of the experiment. Interestingly, the rate of flux within the corona varied depending upon the metabolite in question. A number of metabolites showed an increase in corona composition concentration after just 30 min, whereby 3-methoxytyramine, O-acetyl-L-serine, and serotonin levels increased by 5, 52, and 81%, respectively, demonstrating that corona evolution begins almost immediately following the formation of the metabolite corona. These findings reflect what is already known for the protein corona, and it is the first demonstration of temporal evolution of the metabolite corona. Other metabolites such as 5-hydroxylysine, ornithine, tyramine, arginine, anserine, and methoxy-L-tyrosine only started to show changes following an additional 30 min of incubation, gaining 61, 33, 17, 26, 13, and 4%, respectively, over the course of 1 h. This could suggest that these metabolites have a lower affinity for the uncapped TiO₂ NM surface, or it is possible that they require the rapidly adsorbing metabolites to sufficiently change the surface chemistry of the NMs in order to promote their adsorption. Alongside the different rates of exchange, the desorption extent of each metabolite varied greatly over the full 90 min span, and the range of change over 90 min was 11–91%, not only indicating that the metabolite corona contains a unique metabolite fingerprint, which is well described in the literature,^{7,9–11} but

also suggesting that the rate and extent of change of metabolites in the corona is unique to the metabolite and NM in question, and as noted above, it will also be affected by the pH and ionic strength of the incubation medium or biofluid. Further work to assess binding energies or the impact of addition of new metabolites to the incubation mixes is required to determine the precise mechanisms involved in the recruitment of the metabolite corona, i.e., direct interaction with the NM surface or interaction with another metabolite already attached to the NM surface as part of the initially acquired metabolite corona.

3.6. Application to Other Nanomaterials

In order to determine if the method developed and optimized for recovery and quantification of cationic and anionic metabolites acquired by uncapped TiO₂ and TiO₂-PVP, respectively, was applicable to other NMs, further two NMs were analyzed, namely, Dispex-capped TiO₂ and Fe₃O₄. These NMs were chosen in order to evaluate the difference in recovery based upon particle surface chemistry, uncapped versus Dispex-capped, and NM composition TiO₂ versus Fe₃O₄.

Initially, the recovery of the cationic metabolites was assessed using the pH-optimized 10 mM ammonium formate. To ensure that the results were not skewed by faltering recovery due to only a minimal amount for metabolite adsorbed to the NM corona, only metabolites where at least 20% of the available metabolite adsorbed to one of the three NMs were included in the analysis. It is apparent from Figure 4

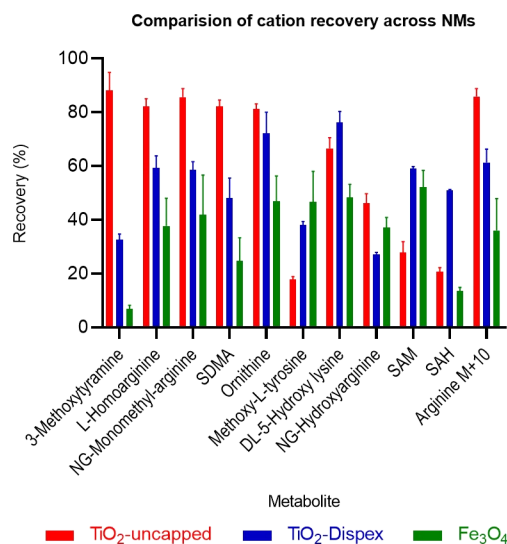


Figure 4. Comparison of the recovery of cations from the three NMs using a recovery method for cations previously optimized using the uncapped TiO₂ NMs.

that there are clear differences in recovery performance between the three NMs. The recovery of cations from the uncapped TiO₂ NMs for which this method was optimized performed significantly better ($p < 0.05$) than the Dispex-capped TiO₂ NMs for five of the cations. The method proved to have significantly greater recoveries ($p < 0.05$) for uncapped TiO₂ compared to Fe₃O₄ for 55% of the cations. The recovery for TiO₂-DISPEX and Fe₃O₄ was only significantly ($p < 0.05$) better than the uncapped TiO₂ NMs for a total of four cations; the recovery from TiO₂-DISPEX significantly ($p < 0.05$) outperformed Fe₃O₄ for 73% of the cations. The fact that the

recoveries from the two TiO₂ NMs are better than those from Fe₃O₄ suggests that the core material plays a significant role in the recovery, while the surface chemistry also seems to be significant in the recovery of metabolites from the corona based upon the uncapped vs Dispex-capped TiO₂.

Interestingly, in the case of the anions (Figure 5), the differences between the PVP and Dispex-capped TiO₂ NMs

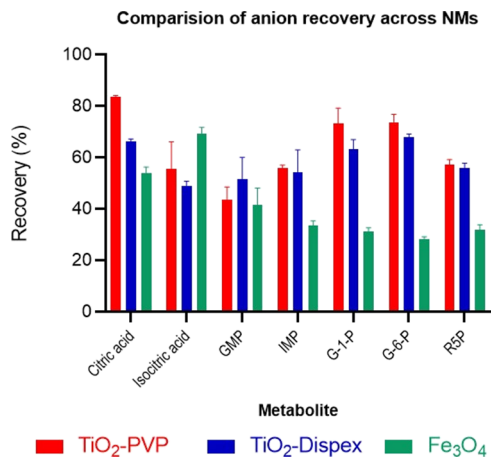


Figure 5. Comparison of the recovery of anions from the three NMs using the recovery method for anions previously optimized using the PVP-capped TiO₂ NMs.

were less pronounced; however, this could be a property of the small number of anions being studied and the similarity of their chemical properties. However, the recovery of the three sugar phosphates from the Fe₃O₄ NMs was significantly lower ($p < 0.001$) than that from the two TiO₂ NMs. It is also interesting to note that the differences between the citric and isocitric acid remain for the two TiO₂ NMs, whereas for Fe₃O₄, the recovery of the isocitric was better than that of citrate. However, with the G-1-P and G-6-P, the isomer patterns were retained across all three NMs. This finding adds further

evidence that the adsorption and desorption kinetics of isomers may also help to elucidate the mechanism of metabolite corona formation.

The significant differences in the recovery efficiencies across all the assessed NMs highlight the importance of performing extensive method optimization for each NM being investigated in a metabolite corona study. To assume that the recovery of one metabolite or one NM can be applied to others runs the significant risk of skewing the data and leading to misinterpretation of the NM metabolite corona. For example, it is possible that an apparent lower concentration of metabolites in a NM corona could be due to a less-efficient recovery of the corona rather than a genuine difference in the corona composition.

3.7. Incubation of NMs and Cationic Metabolites with Intact Human Plasma

In all biological matrices, polar metabolites coexist with other components, such as lipids and proteins, and it has been shown that the difference in matrices could lead to varying interaction characteristics between NMs and polar metabolites.¹⁰ In light of the coexistence of lipids and proteins in the NM coronas formed in biological matrices,^{21,40,41} it is of great importance to evaluate the effectiveness of the proposed elution procedure in recovering polar metabolites from the more complex “biomolecule corona”. In this work, intact pooled human plasma was chosen to provide a biological environment, and the cationic standard solution was spiked into the incubation mix for evaluation of the effectiveness of the wash procedure to recover the cations.

Two experimental set-ups were included for this evaluation, detailed in Table S3, and based on the concentration differences of the incubation components, the two groups are referred to as the low-concentration group and high-concentration group separately. The collected data were first compiled, and the fluctuation of metabolite responses, expressed as RSD, was calculated. It was revealed that 44 of the 45 cations from the QC samples showed RSD values below 25% acquired from the low-composition group, and 42 of 45

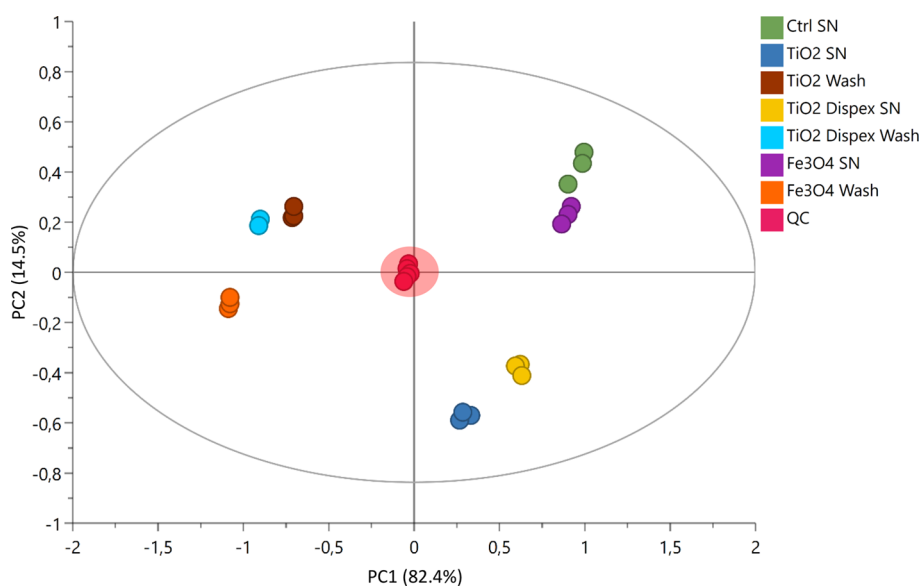


Figure 6. PCA plot generated for normalized peak areas of cations observed in the incubation experiment with 1 mg/mL NM, 2.5 μM cation mix, and 5 μL of human plasma. The ISTD used for normalization is *N*-methyl-d₃-L-histidine. The quality of the analysis is represented by the quality control (QC) samples clustering in the unsupervised PCA-X plot model.

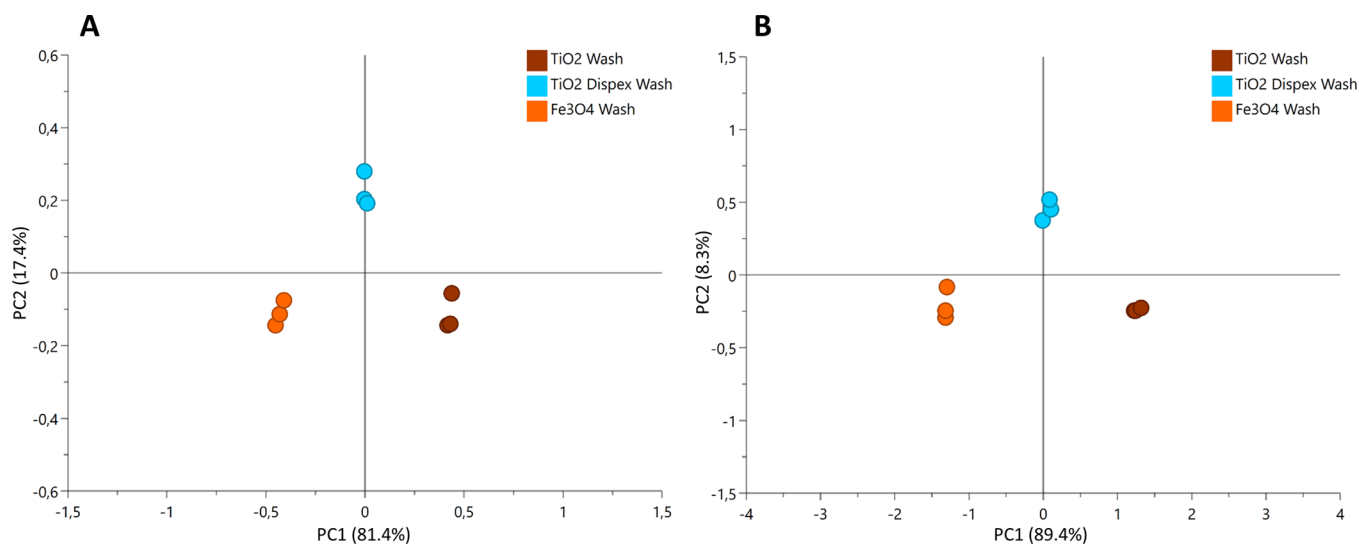


Figure 7. PCA plots generated for only the elution fraction samples obtained for two different incubation schemes. (A) Incubation mix contains 1 mg/mL NM, 2.5 μ M cation mix, and 5 μ L of human plasma. (B) Incubation mix contains 5 mg/mL NM, 12.5 μ M cations, and 10 μ L of human plasma. Ammonium formate (10 mM) was used for eluting after incubation in both experiments.

cations met this requirement in the high-composition group. Before conducting multivariate analyses using the SIMCA software, it was noticed that, despite the overall stability of peak areas across the sequence, the responses of ISTDs in a few samples were much lower than the rest. To eliminate such fluctuations, peak areas were normalized with *N*-methyl-d3-*L*-histidine and the obtained peak area ratios were subjected to further data analysis with SIMCA. The imported area ratios were first subjected to Pareto scaling, and the number of significant components was determined with Autofit. As shown in the principal component analysis (PCA) plot (Figure 6), the QC samples were clustered in the center, suggesting excellent analytical stability throughout the sequence, while supernatant samples (unbound cations) and elution samples (metabolites recovered from the NMs) were spread on opposing sides of the QCs, indicating their clear differences. Notably, the supernatant samples from control samples and Fe₃O₄ NM incubation mix are clustering closely, reflecting the relatively low adsorption of metabolites to the Fe₃O₄ NM, which is in accordance with the results acquired when incubated in H₂O. On the other hand, localization was demonstrated for TiO₂ and TiO₂-DISPEX NMs in the supernatant and elution fraction samples, respectively, which can be attributed to the NM structural similarity. The same separation pattern was also observed for the high-composition group (Figure S1).

In our previous work, the differences among NM (polar) metabolite coronas have mainly been illustrated based on the extent of metabolite depletion from the supernatant after incubation.¹⁰ To check whether the elution fractions also show NM-dependent behaviors using the proposed recovery process, PCA plots with all the elution fraction samples from both plasma-included incubation experiments were generated (Figure 7). As can be seen from the plots, the three groups of elution fractions were clustered and positioned similarly in both incubation experiments, which suggests that the proposed elution procedure can retain NM-specific information in the elution fractions despite the change of the experimental composition of the exposure biofluid. Subsequently, partial least squares discriminant analysis (PLS-DA) was conducted and variable importance in projection (VIP) scores were

summarized to pinpoint compounds that led to such separation. For both plasma-included incubation studies, two groups of highly similar compounds were responsible for the separation observed with PLS-DA plots (VIP value > 1, Table S5), with one extra cation confirmed for the low-composition NM incubation. Interestingly, among all the compounds with a VIP score over 1.0, both groups contained seven compounds that are arginine or arginine derivatives, with wash samples from TiO₂ NM incubations showing significantly higher absolute recovery ($p < 0.01$) for almost all of them (with the exception of NG-hydroxyarginine in the high-composition incubation). The Fe₃O₄ NM, of the three NMs assessed, demonstrated the lowest overall absolute recovery in the elution fraction samples, which is in perfect alignment with its highest overall absolute amounts remaining in the supernatant after incubation. The results presented here not only emphasize the usefulness of the proposed elution procedure, but more importantly, they also offer a unique approach in studying NM-dependent metabolite coronas.

4. CONCLUSIONS

This study is the first to demonstrate the importance of careful methodical sample preparation for the isolation of the metabolite corona acquired by NMs. We demonstrate that both the pH and ionic strength of the elution buffer have significant effects on the recovery of both cations and anions. The method developed and optimized for uncapped TiO₂ NMs was used to demonstrate that the metabolite corona undergoes dynamic evolution over time suggesting that the incubation period in metabolite corona studies may have important implications on the outcome of the study. We also show that it is important to perform suitable method development and optimization of separation conditions (buffer pH, ionic strength, and incubation time) for each nanomaterial in a particular study as both the elemental composition and surface chemistry impact the ability to reliably isolate the metabolites that have adsorbed into the NM corona. Full documentation of all steps and conditions and their impact on recovery is also recommended to facilitate repeatability and replication.

■ ASSOCIATED CONTENT

SI Supporting Information

The Supporting Information is available free of charge at <https://pubs.acs.org/doi/10.1021/acsmesuresciau.2c00003>.

Metabolite physical and chemical properties, NM characteristics, elution volume on recovery, experimental set-up, and multivariate statistics (PDF)

■ AUTHOR INFORMATION

Corresponding Authors

Wei Zhang – Leiden Academic Centre for Drug Research, Leiden University, 2333CC Leiden, The Netherlands; orcid.org/0000-0002-8320-3959; Email: w.zhang@lacdr.leidenuniv.nl

Andrew J. Chetwynd – School of Geography, Earth and Environmental Sciences, University of Birmingham, Birmingham B15 2TT, U.K.; Department of Women's and Children's Health, Institute of Life Course and Medical Sciences, University of Liverpool, Liverpool L12 2AP, U.K.; orcid.org/0000-0001-6648-6881; Email: a.j.chetwynd@liverpool.ac.uk

Authors

James A. Thorn – AB SCIEX UK Ltd., SCIEX UK Centre of Innovation, Cheshire SK10 4TG, U.K.

Iseult Lynch – School of Geography, Earth and Environmental Sciences, University of Birmingham, Birmingham B15 2TT, U.K.; orcid.org/0000-0003-4250-4584

Rawi Ramautar – Leiden Academic Centre for Drug Research, Leiden University, 2333CC Leiden, The Netherlands; orcid.org/0000-0002-1673-4848

Complete contact information is available at: <https://pubs.acs.org/doi/10.1021/acsmesuresciau.2c00003>

Notes

The authors declare no competing financial interest.

■ ACKNOWLEDGMENTS

A.J.C., I.L., and J.A.T. acknowledge funding from the European Commission via Horizon 2020 project ACEnano (Grant no. H2020-NMBP-2016-720952). W.Z. and R.R. acknowledge the financial support of the Vidi grant scheme of the Netherlands Organization of Scientific Research (NWO Vidi 723.016.003).

■ REFERENCES

- (1) Ke, P. C.; Lin, S.; Parak, W. J.; Davis, T. P.; Caruso, F. A Decade of the Protein Corona. *ACS Nano* **2017**, *11*, 11773–11776.
- (2) Lynch, I.; Dawson, K. A. Protein-Nanoparticle Interactions. *Nano Today* **2008**, *3*, 40–47.
- (3) Wheeler, K. E.; Chetwynd, A. J.; Fahy, K. M.; Hong, B. S.; Tochihiuti, J. A.; Foster, L. A.; Lynch, I. Environmental Dimensions of the Protein Corona. *Nat. Nanotechnol.* **2021**, 617–629.
- (4) Lynch, I.; Feitshans, I. L.; Kendall, M. 'Bio-Nano Interactions: New Tools, Insights and Impacts': Summary of the Royal Society Discussion Meeting. *Philos. Trans. R. Soc., B* **2015**, *370*, No. 20140162.
- (5) Griffith, D. M.; Jayaram, D. T.; Spencer, D. M.; Pisetsky, D. S.; Payne, C. K. DNA-Nanoparticle Interactions: Formation of a DNA Corona and Its Effects on a Protein Corona. *Biointerphases* **2020**, *15*, No. 051006.

- (6) Gardner, L.; Warrington, J.; Rogan, J.; Rothwell, D. G.; Brady, G.; Dive, C.; Kostarelou, K.; Hadjidemetriou, M. The Biomolecule Corona of Lipid Nanoparticles Contains Circulating Cell-Free DNA. *Nanoscale Horiz.* **2020**, *5*, 1476–1486.

- (7) Lee, J. Y.; Wang, H.; Pyrgiotakis, G.; DeLoid, G. M.; Zhang, Z.; Beltran-Huarac, J.; Demokritou, P.; Zhong, W. Analysis of Lipid Adsorption on Nanoparticles by Nanoflow Liquid Chromatography-Tandem Mass Spectrometry. In *Analytical and Bioanalytical Chemistry*; Springer: Berlin Heidelberg, 2018; pp. 1–10.

- (8) Müller, J.; Prozeller, D.; Ghazaryan, A.; Kokkinopoulou, M.; Mailänder, V.; Morsbach, S.; Landfester, K. Beyond the Protein Corona – Lipids Matter for Biological Response of Nanocarriers. *Acta Biomater.* **2018**, *71*, 420–431.

- (9) Pink, M.; Verma, N.; Kersch, C.; Schmitz-Spanke, S. Identification and Characterization of Small Organic Compounds within the Corona Formed around Engineered Nanoparticles. *Environ. Sci. Nano* **2018**, *5*, 1420–1427.

- (10) Chetwynd, A. J.; Zhang, W.; Thorn, J. A.; Lynch, I.; Ramautar, R. The Nanomaterial Metabolite Corona Determined Using a Quantitative Metabolomics Approach: A Pilot Study. *Small* **2020**, *16*, No. 2000295.

- (11) Grintzalis, K.; Lawson, T. N.; Nasser, F.; Lynch, I.; Viant, M. R. Metabolomic Method to Detect a Metabolite Corona on Amino Functionalised Polystyrene Nanoparticles. *Nanotoxicology* **2019**, 1–12.

- (12) Martel, J.; Wu, C. Y.; Hung, C. Y.; Wong, T. Y.; Cheng, A. J.; Cheng, M. L.; Shiao, M. S.; Young, J. D. Fatty Acids and Small Organic Compounds Bind to Mineralo-Organic Nanoparticles Derived from Human Body Fluids as Revealed by Metabolomic Analysis. *Nanoscale* **2016**, *8*, 5537–5545.

- (13) Chetwynd, A. J.; Lynch, I. The Rise of the Nanomaterial Metabolite Corona, and Emergence of the Complete Corona. *Environ. Sci. Nano* **2020**, *7*, 1041–1060.

- (14) Ruge, C. A.; Schaefer, U. F.; Herrmann, J.; Kirch, J.; Cañadas, O.; Echaide, M.; Pérez-Gil, J.; Casals, C.; Müller, R.; Lehr, C. M. The Interplay of Lung Surfactant Proteins and Lipids Assimilates the Macrophage Clearance of Nanoparticles. *PLoS One* **2012**, *7*, e40775.

- (15) Zhang, X.; Pandiakumar, A. K.; Hamers, R. J.; Murphy, C. J. Quantification of Lipid Corona Formation on Colloidal Nanoparticles from Lipid Vesicles. *Anal. Chem.* **2018**, *90*, 14387–14394.

- (16) Faria, M.; Björnmalm, M.; Thurecht, K. J.; Kent, S. J.; Parton, R. G.; Kavallaris, M.; Johnston, A. P. R.; Gooding, J. J.; Corrie, S. R.; Boyd, B. J.; et al. Minimum Information Reporting in Bio-Nano Experimental Literature. *Nat. Nanotechnol.* **2018**, *13*, 777–785.

- (17) Leong, H. S.; Butler, K. S.; Brinker, C. J.; Azzawi, M.; Conlan, S.; Dufés, C.; Owen, A.; Rannard, S.; Scott, C.; Chen, C.; et al. On the Issue of Transparency and Reproducibility in Nanomedicine. *Nat. Nanotechnol.* **2019**, *14*, 629–635.

- (18) Chetwynd, A. J.; Wheeler, K. E.; Lynch, I. Best Practice in Reporting Corona Studies: Minimum Information about Nanomaterial Biocorona Experiments (MINBE). *Nano Today* **2019**, *28*, 100758.

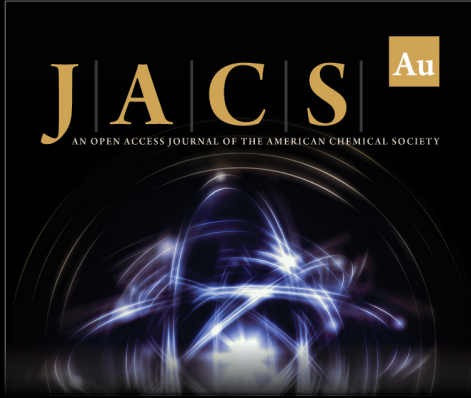
- (19) Chetwynd, A. J.; Dunn, W. B.; Rodriguez-Blanco, G. Collection and Preparation of Clinical Samples for Metabolomics. In *Advances in Experimental Medicine and Biology*; 2017; Vol. 965, pp 19–44.

- (20) Zhang, H.; Burnum, K. E.; Luna, M. L.; Petritis, B. O.; Kim, J. S.; Qian, W. J.; Moore, R. J.; Heredia-Langner, A.; Webb-Robertson, B. J. M.; Thrall, B. D.; et al. Quantitative Proteomics Analysis of Adsorbed Plasma Proteins Classifies Nanoparticles with Different Surface Properties and Size. *Proteomics* **2011**, *11*, 4569–4577.

- (21) Faserl, K.; Chetwynd, A. J.; Lynch, I.; Thorn, J. A.; Lindner, H. H. Corona Isolation Method Matters: Capillary Electrophoresis Mass Spectrometry Based Comparison of Protein Corona Compositions Following On-Particle versus In-Solution or In-Gel Digestion. *Nanomaterials* **2019**, *9*, 898.


- (22) Docter, D.; Distler, U.; Storck, W.; Kuharev, J.; Wünsch, D.; Hahlbrock, A.; Knauer, S. K.; Tenzer, S.; Stauber, R. H. Quantitative Profiling of the Protein Coronas That Form around Nanoparticles. *Nat. Protoc.* **2014**, *9*, 2030–2044.


- (23) Tenzer, S.; Docter, D.; Kuharev, J.; Musyanovych, A.; Fetz, V.; Hecht, R.; Schlenk, F.; Fischer, D.; Kiouptsi, K.; Reinhardt, C.; et al. Rapid Formation of Plasma Protein Corona Critically Affects Nanoparticle Pathophysiology. *Nat. Nanotechnol.* **2013**, *8*, 772–781.
- (24) Gulersonmez, M. C.; Lock, S.; Hankemeier, T.; Ramautar, R. Sheathless Capillary Electrophoresis-Mass Spectrometry for Anionic Metabolic Profiling. *Electrophoresis* **2016**, *37*, 1007–1014.
- (25) Ramautar, R.; Somsen, G. W.; de Jong, G. J. CE-MS in Metabolomics. *Electrophoresis* **2009**, *30*, 276–291.
- (26) Zhang, W.; Guled, F.; Hankemeier, T.; Ramautar, R. Profiling Nucleotides in Low Numbers of Mammalian Cells by Sheathless CE-MS in Positive Ion Mode: Circumventing Corona Discharge. *Electrophoresis* **2020**, *41*, 360–369.
- (27) Zhang, W.; Ramautar, R. CE-MS for Metabolomics: Developments and Applications in the Period 2018–2020. *Electrophoresis* **2020**, *42*, 381–401.
- (28) Chetwynd, A. J.; Guggenheim, E. J.; Briffa, S. M.; Thorn, J. A.; Lynch, I.; Valsami-Jones, E. Current Application of Capillary Electrophoresis in Nanomaterial Characterisation and Its Potential to Characterise the Protein and Small Molecule Corona. *Nanomaterials* **2018**, *8*, 99.
- (29) Chetwynd, A. J.; Zhang, W.; Faserl, K.; Thorn, J. A.; Lynch, I.; Ramautar, R.; Lindner, H. H. Capillary Electrophoresis Mass Spectrometry Approaches for Characterization of the Protein and Metabolite Corona Acquired by Nanomaterials. *J. Visualized Exp.* **2020**, *164*, 61760.
- (30) Drouin, N.; van Mever, M.; Zhang, W.; Tobolkina, E.; Ferre, S.; Servais, A.-C.; Gou, M.-J.; Nyssen, L.; Fillet, M.; Lageveen-Kammeijer, G. S. M.; et al. Capillary Electrophoresis-Mass Spectrometry at Trial by Metabo-Ring: Effective Electrophoretic Mobility for Reproducible and Robust Compound Annotation. *Anal. Chem.* **2020**, *92*, 14103–14112.
- (31) Khan, A. O.; Di Maio, A.; Guggenheim, E. J.; Chetwynd, A. J.; Pencross, D.; Tang, S.; Belinga-Desaunay, M.-F. A.; Thomas, S. G.; Rappoport, J. Z.; Lynch, I. Surface Chemistry-Dependent Evolution of the Nanomaterial Corona on TiO₂ Nanomaterials Following Uptake and Sub-Cellular Localization. *Nanomaterials* **2020**, *10*, 401.
- (32) Wishart, D. S.; Feunang, Y. D.; Marcu, A.; Guo, A. C.; Liang, K.; Vázquez-Fresno, R.; Sajed, T.; Johnson, D.; Li, C.; Karu, N.; et al. HMDB 4.0: The Human Metabolome Database for 2018. *Nucleic Acids Res.* **2018**, *46*, D608–D617.
- (33) Zhang, W.; Gulersonmez, M. C.; Hankemeier, T.; Ramautar, R. Sheathless Capillary Electrophoresis–Mass Spectrometry for Metabolic Profiling of Biological Samples. *J. Visualized Exp.* **2016**, *2016*, e54535.
- (34) Vuckovic, D.; Pawliszyn, J. Systematic Evaluation of Solid-Phase Microextraction Coatings for Untargeted Metabolomic Profiling of Biological Fluids by Liquid Chromatography-Mass Spectrometry. *Anal. Chem.* **2011**, *83*, 1944–1954.
- (35) Maranata, G. J.; Surya, N. O.; Hasanah, A. N. Optimising Factors Affecting Solid Phase Extraction Performances of Molecular Imprinted Polymer as Recent Sample Preparation Technique. *Heliyon* **2021**, *7*, e05934.
- (36) Bergés, R.; Sanz-Nebot, V.; Barbosa, J. Modelling Retention in Liquid Chromatography as a Function of Solvent Composition and PH of the Mobile Phase. *J. Chromatogr. A* **2000**, *869*, 27–39.
- (37) Lundqvist, M.; Stigler, J.; Cedervall, T.; Berggård, T.; Flanagan, M. B.; Lynch, I.; Elia, G.; Dawson, K. The Evolution of the Protein Corona around Nanoparticles: A Test Study. *ACS Nano* **2011**, *5*, 7503–7509.
- (38) Casals, E.; Pfaller, T.; Duschl, A.; Oostingh, G. J.; Puentes, V. Time Evolution of the Nanoparticle Protein Corona. *ACS Nano* **2010**, *4*, 3623–3632.
- (39) Walkey, C. D.; Chan, W. C. W. Understanding and Controlling the Interaction of Nanomaterials with Proteins in a Physiological Environment. *Chem. Soc. Rev.* **2012**, *41*, 2780–2799.
- (40) Lima, T.; Bernfur, K.; Vilanova, M.; Cedervall, T. Understanding the Lipid and Protein Corona Formation on Different Sized Polymeric Nanoparticles. *Sci. Rep.* **2020**, *10*, 1129.
- (41) La Barbera, G.; Capriotti, A. L.; Caracciolo, G.; Cavaliere, C.; Cerrato, A.; Montone, C. M.; Piovesana, S.; Pozzi, D.; Quagliarini, E.; Laganà, A. A Comprehensive Analysis of Liposomal Biomolecular Corona upon Human Plasma Incubation: The Evolution towards the Lipid Corona. *Talanta* **2020**, *209*, No. 120487.



JACS Au
AN OPEN ACCESS JOURNAL OF THE AMERICAN CHEMICAL SOCIETY

Editor-in-Chief
Prof. Christopher W. Jones
Georgia Institute of Technology, USA

Open for Submissions 

pubs.acs.org/jacsau  ACS Publications
Most Trusted. Most Cited. Most Read.